Atmos. Chem. Phys. Discuss., 15, 11111–11141, 2015
www.atmos-chem-phys-discuss.net/15/11111/2015/
doi:10.5194/acpd-15-11111-2015

Atmospheric Chemistry and Physics Discussions

Heavy air pollution episodes in Beijing during January 2013: inorganic ion chemistry and source analysis using Highly Time-Resolved Measurements in an urban site

B. Han[1], R. Zhang[1,2], W. Yang[1], Z. Bai[1], Z. Ma[3], and W. Zhang[1]

[1]State Key Laboratory of Environmental Criteria and Risk Assessment, Chinese Research Academy of Environmental Sciences, Beijing, China
[2]Beijing Municipal Research Institute of Environmental Protection, Beijing, China
[3]Institute of Urban Meteorology, China Meteorological Administration, Beijing, China

Received: 11 March 2015 – Accepted: 17 March 2015 – Published: 15 April 2015

Correspondence to: Z. Bai (baizp@craes.org.cn)

Published by Copernicus Publications on behalf of the European Geosciences Union.

Abstract

Heavy air pollution episodes occurred in Beijing in January 2013 attracted intensively attention around the whole world. During this period, the authors conducted highly time-resolved measurements of water soluble ions associated with $PM_{2.5}$ at an urban site, and attempted to distinguish the ion chemistry and potential sources. In this study, hourly mean concentrations of Cl^-, NO_3^-, SO_4^{2-}, Na^+, NH_4^+, K^+, Mg^{2+} and Ca^{2+} were measured during the air pollution episode in January 2013, and the ions were found to exist mainly in the form of $(NH_4)_2SO_4$, NH_4NO_3, NaCl and KCl in aerosol particles by correlation and linear analysis. SO_4^{2-} and NO_3^- were observed peak concentrations in 10–15, 18–20, 21–24, and 26–30 January during this monitoring campaign. The percentage of SO_4^{2-} and NH_4^+ in total ions concentrations exhibited an increasing trend with the enhancement of $PM_{2.5}$ concentration, indicating high concentrations of SO_4^{2-} and NH_4^+ had played important roles in the formation of air pollution episodes. Ratio of $[NO_3^-]/[SO_4^{2-}]$ was calculated, finding the sources of SO_4^{2-} would contribute more to the formation of $PM_{2.5}$ than mobile sources. Diurnal variations of SO_4^{2-}, NO_3^-, NH_4^+ were examined, and all of them exhibited similar pattern with high concentration in night and relative low level at daytime. Emission from coal combustion, remote transportation at night or impact of meteorological was likely to be responsible for the high level of SO_4^{2-}, NH_4^+ and NO_3^-. Potential sources were identified by applying PMF. Secondary nitrate, secondary sulfate, coal combustion and biomass burning, as well as fugitive dust were considered as the major contributors to total ions.

1 Introduction

As the capital of China, Beijing (39.9° N, 116.4° E) has more than 20 million inhabitants distributed over 16 800 km^2. The city has been facing serious air pollution. During the past two decades, Beijing experienced a rapid increase and development in en-

ACPD
15, 11111–11141, 2015

ergy consumption, vehicle quantities and urban expansion, plus the fugitive dust from surrounding soil or constructive activities.

Since 2000, air pollution control measures have been designed and taken to reduce local emission and improve air quality. However, after 2008 Olympic Games, the regional pollution and visibility in the whole area has become worsen (Zhang et al., 2010) and serious air pollution episodes occurred frequently (Cao et al., 2012; Huang et al., 2010; Sun et al., 2013; Wang et al., 2009). High concentration of $PM_{2.5}$ was believed to be largely responsible for the deterioration of air quality and visibility. With the implementation of China's new National Ambient Air Quality Standard for $PM_{2.5}$ in 2012, more challenges arose to improve air quality in megacities (Hu et al., 2014).

Some previous studies found secondary inorganic aerosol (SIA), such as sulfate, nitrate and ammonium were the dominant ions in atmospheric $PM_{2.5}$ of Beijing (Cao et al., 2012; Duan et al., 2003; Pathak et al., 2009; Yao et al., 2002). These components have effects on the hygroscopicity and acidity of aerosol, which are important factors in influencing aerosol-phase chemistry and uptake of gaseous species by particles (Ocskay et al., 2006; Xue et al., 2011; Shon et al., 2012). He et al. (2001) and Ye et al. (2003) reported SO_4^{2-}, NO_3^-, and NH_4^+ accounted for about one-third of the total $PM_{2.5}$ mass in Shanghai and Beijing. Yao et al. (2002) investigated the formation of SO_4^{2-} and NO_3^- in $PM_{2.5}$ in understanding the origin of these species. They found that a large part of these species might be formed through the direct emissions of SO_2, NO_x, and NH_3. Wang et al. (2005) collected daily $PM_{2.5}$ aerosol samples at five sites in Beijing for a 3 year period from 2001 to 2003, and analyzed concentrations of the water-soluble ions, finding that the inorganic ions existed mainly in the form of $(NH_4)_2SO_4$, NH_4NO_3, NaCl, KCl, and $CaCl_2$ in aerosol particles. Zhang et al. (2013) collected daily $PM_{2.5}$ samples between April 2009 and January 2010 at Beijing, finding SO_4^{2-} ranked the highest among the water-soluble ions analyzed, with an annual mean of $13.6 \pm 12.4\,\mu g\,m^{-3}$, followed by NO_3^- ($11.3 \pm 10.8\,\mu g\,m^{-3}$), NH_4^+ ($6.9 \pm 7.1\,\mu g\,m^{-3}$), Ca^{2+} ($1.6 \pm 1.4\,\mu g\,m^{-3}$), Cl^- ($1.4 \pm 2.2\,\mu g\,m^{-3}$), K^+ ($0.92 \pm 0.75\,\mu g\,m^{-3}$), Na^+ ($0.46 \pm 0.55\,\mu g\,m^{-3}$), and Mg^{2+} ($0.16 \pm 0.13\,\mu g\,m^{-3}$).

ACPD
15, 11111–11141, 2015

Most of previous studies used filter-based methods to collect PM samples with each sample covering hours to days. Such low temporal resolution data have limitations when used for investigating secondary aerosol formation and time evolution. Highly time-resolved measurements were considered to be helpful for a wide range of $PM_{2.5}$ components, including inorganic compounds. Data from the high resolution instruments offer significant advantages over traditional 24 h integrated filter-based measurements (Vedantham et al., 2014). To investigate the impacts of control measures and regional transport in 2008 Olympic Games, Gao et al. (2013) conducted highly time-resolved measurements of SO_4^{2-}, NO_3^-, and NH_4^+ in $PM_{2.5}$ simultaneously at an urban site and a downwind rural site in Beijing during the 2008 Olympics. The mean concentrations of SO_4^{2-}, NO_3^-, and NH_4^+ were 18.23, 9.47, and 9.70 $\mu g\,m^{-3}$, respectively, at the rural site and 20.74, 8.83, and 10.85 $\mu g\,m^{-3}$, respectively, at the urban site. Hu et al. (2014) monitored hourly water-soluble inorganic ions in $PM_{2.5}$ and gaseous precursors during June–November 2009 at an urban site in Beijing. The average mass concentration of the total water-soluble ions was 44 $\mu g\,m^{-3}$, accounting for 38 % of $PM_{2.5}$. SO_4^{2-}, NO_3^-, and NH_4^+ were dominant ions.

In the first beginning to 2013, Beijing's January air pollution episodes drew international media attention. Beijing, along with the rest of the mideastern region of China, experienced massive, severe air pollution episodes (Ouyang, 2013).

The high concentration of $PM_{2.5}$ was believed to be largely responsible for the deterioration of air quality and visibility. Five haze pollution episodes were identified in the Beijing-Tianjin-Hebei area, with the two most severe episodes occurring during 9–15 and 25–31 January. During these two haze pollution episodes, the maximum hourly $PM_{2.5}$ mass concentrations in Beijing were 680 and 530 $\mu g\,m^{-3}$, respectively (Wang et al., 2014a). As urgent countermeasure, some industries and construction activities were suspended. Heavy air pollution episode also aroused some adverse health effects. The term "Beijing cough" has been in use since as early as the 1990s among foreigners, many of whom experienced chronic respiratory problems when they arrived in Beijing due to the city's dry and polluted air. But it did not become well-known un-

ACPD
15, 11111–11141, 2015

til recently, when more health problems directly attributable to the current heavy air pollution (Chen et al., 2013).

By now, there have been several studies related on the occurring of these heavy pollution episodes in Beijing. Wang et al. (2014a) and Ji et al. (2014) analyzed the mechanism for the formation of heavy pollution episode, concluding that the external cause of the severe haze episodes was the unusual atmospheric circulation, the depression of strong cold air activities and the very unfavorable dispersion due to geographical and meteorological conditions, and internal cause was the quick secondary transformation of primary gaseous pollutants to secondary aerosols. Secondary aerosol was considered as one of the most important reasons of heavy air pollution episodes. Wang et al. (2014a) also revealed the two stage of aerosol growth. i.e. the "explosive growth" and "sustained growth". Huang et al. (2014) found anomalous meteorological conditions in 2013, which was different from the normal climatology from 2007–2012, were especially favorable for haze formation, and explained the formation mechanism of this episode in regard of aerosol chemistry based on the field measurement and meteorological analysis during the first half of January 2013. Zhang et al. (2014) achieved the similar conclusion that anomalous meteorology was found for this long-lasting air pollution episode, explaining about 2/3 of the variance of daily visibility evolution. Model simulation indicated that regional transport played an important role in the formation of regional haze over the Beijing-Tianjin-Heibei area (Wang et al., 2014b)

To better understand the compositions of $PM_{2.5}$ and their impact on air quality in the heavy air pollution episodes during January 2013, this study analyzed the highly time-resolved measurements of inorganic ions associated with $PM_{2.5}$, and investigated the characteristics of aerosol inorganic ions, major chemical forms, as well as potential sources. Different from previous studies which paid close attention to meteorological analysis, this paper mainly focused on specific ion compositions, which was considered as one of the major contributor to air pollution episode, and had an in-deep discussion on their role in forming the episode. The paper will help us have a more comprehensive understanding of air pollution episode in Beijing.

ACPD
15, 11111–11141, 2015

2 Experimental

2.1 Sampling sites and meteorological conditions

The field campaign was conducted in the January 2013, and the sampling site was on the rooftop of a building in the Chinese Research Academy of Environmental Sciences (CRAES, 40°2′29.46″ N, 116°24′51.00″ E), which is located outside the 4 km north of the 5th Ring Road and 15 km from the city center as shown in Fig. 1.

The wind rose of Beijing in January is depicted in Fig. 2, and the corresponding calm wind frequencies are listed in Table 1. Firstly, the prevailing wind directions (frequency higher than 10 %) were SW (12.50 %), ENE (11.33 %), N (10.94 %) and WSW (10.74 %). Compared with the statistical results of Zhao et al. (2013) for 2009 and 2010, the frequency of WSW, SW and SSW were higher in this study. Su et al. (2004) concluded that southwest transport pathway was one of the three major pathways for outside pollutants being transported to Beijing. The CMAQ model simulation of secondary aerosols around Beijing in summer of 2003 by Liu et al. (2005) suggested that when wind from southern and southwestern directions prevails in Beijing, high concentrations of vapor and NH_3 was brought in, which would enhanc the efficiency of the secondary aerosol production. Secondly, the average temperature in January 2013 (−5.1 °C) was lower than that in 2009 and 2010 (−2.0 °C) (Zhao et al., 2013). Lower temperature would lead to more demand for fossil fuel, and more air pollutants could be emitted. Thirdly, the calm wind frequency (6.64 %) was higher than that in 2009 and 2010 (3.21 %), which was perhaps an important reason for the air pollution episode in January 2013.

2.2 Instruments

The hourly concentrations of Cl^-, NO_3^-, SO_4^{2-}, Na^+, NH_4^+, K^+, Mg^{2+} and Ca^{2+} associated with $PM_{2.5}$ were simultaneously measured by an ambient ion monitor (Model URG 9000B, URG Corporation, USA). This instrument draws air in through a $PM_{2.5}$

ACPD
15, 11111–11141, 2015

sharp-cut cyclone at a volumetric-flow controlled rate of 3 L min^{-1} to remove the larger particles from the air stream. Then the air stream is drawn through a liquid diffusion denuder where water-soluble acid gases (e.g., SO_2, NH_3, and HNO_3) are removed. In order to achieve high collection efficiencies, the particles-laden air stream next enters an aerosol super-saturation chamber to enhance particle growth. An inertial particle separator collects these enlarged particles, which are dissolved in water solution and then injected into the ion chromatograph. The detection limits of ions were shown in Table 2.

Hourly concentrations of $PM_{2.5}$ were obtained from Chaoyang Meteorological Bureau, which is 10 km away from the CRAES sampling site.

2.3 Data analysis

Data were analyzed using SPSS 17.0 for Windows (SPSS Inc., 2008) for the correlation analysis and linear regression. EPA PMF 4.2 (USEPA, 2011) was applied to identify the potential contributors to the ion species. A detailed introduction to Positive Matrix Factorization (PMF) is shown in the Supplement.

3 Results and discussion

3.1 Characterizations of ionic species

Water-soluble ions comprise a large part of aerosol particles and play an important role in the atmosphere. Na^+, Mg^{2+}, and Ca^{2+} are mainly from crustal sources, such as re-suspended road dust, soil dust, and construction dust, and SO_4^{2-}, NO_3^-, and NH_4^+ represent the secondary pollution sources from the transformation of their precursors of NH_3, SO_2 and NO_x (Wang et al., 2005). Cl^- is usually considered to be from coal combustion (He et al., 2001), and K^+ is from biomass burning (Duan et al., 2004).

ACPD
15, 11111–11141, 2015

The concentrations of ionic species in the whole sampling period were shown in Table 3. Hourly concentrations of individual ions from AIM measurements varied significantly in a broad range. Emission intensities of gaseous precursors, oxidation or conversion rate, local atmospheric mixing, and regional transport all would affect their concentration levels (Hu et al., 2014).

Wang et al. (2014a) reported that five air pollution episodes were identified in the Beijing-Tianjin-Hebei (Jing-Jin-Ji) area in this time period, and the two most severe episodes occurred during 9–15 and 25–31 January. This study also analyzed the continuous variations of ions in Fig. 3, finding peak values of SO_4^{2-}, NO_3^- and Cl^- were observed on four periods: 10–15, 18–20, 21–24, and 26–30 January. NH_4^+ and K^+ had only peak concentrations during 10–15 January. Concentrations of Na^+, Ca^{2+} and Mg^{2+} showed no significant variations before 28 January. In the last several days, the concentrations of Ca^{2+} and Mg^{2+} decreased dramatically. Most constructive activities related with the emission of Ca^{2+} and Mg^{2+} were suspended by government during this episode. This would perhaps be the reason of lower concentrations of Ca^{2+} and Mg^{2+} after 28 January.

To better understand the ion species characterizations in January 2013, the main ion concentrations measured by manual sampling in the winter of Beijing from other study were summarized in Table 4. We can find that the concentrations of SO_4^{2-}, NO_3^-, Cl^- and NH_4^+ were comparable in different studies.

Huang et al. (2014) collected $PM_{2.5}$ samples during 4–9 January (light air pollution) and 10–15 January (heavy air pollution), and analyzed daily concentrations of ions. We calculated the mean ions concentrations during corresponding time periods as shown in Table 5. The concentrations of Cl^-, NO_3^-, SO_4^{2-} and NH_4^+ in these two studies are comparable, except the NH_4^+ during light air pollution period (4–9 January). Large differences were observed for some ions with relatively low levels, such as Na^+, K^+, Mg^{2+}, Ca^{2+}.

Chinese Ministry of Environmental Protection promulgated "Technical Regulation on Ambient Air Quality Index (on trial)" in 2012, and regulated the AQI values and corre-

ACPD
15, 11111–11141, 2015

sponding concentrations of air pollutants. The regulation divided the daily concentrations of $PM_{2.5}$ into six classes: 0–35, 35–75, 75–115, 115–150, 150–250 and larger than 250 $\mu g\,m^{-3}$, corresponding AQI as follows: 0–50 (excellent), 51–100 (good), 101–150 (light pollution), 151–200 (medium pollution), 201–300 (heavy pollution) and more than 300 (severe pollution). According to the $PM_{2.5}$ concentration classification, this study divided the ions concentrations into six categories and compared their distribution trend in Fig. 4. Except Mg^{2+} and Ca^{2+}, all ions concentrations showed an increasing trend with the deterioration of $PM_{2.5}$ pollution, indicating the ion species (except Mg^{2+} and Ca^{2+}) contributed to the increase of $PM_{2.5}$ concentration.

To further investigate the relative abundance variation trend, percentage of ion species in different $PM_{2.5}$ concentration ranges were calculated as shown in Fig. 5. Cl^-, NO_3^-, Na^+, K^+, Mg^{2+} and Ca^{2+} showed a declining trend along with the increase of $PM_{2.5}$ levels, while SO_4^{2-} and NH_4^+ took up increasing proportions of total ions (the increasing of NH_4^+ abundance was not significant, from 12.7 % under the $PM_{2.5}$ concentration less than 35 $\mu g\,m^{-3}$ to 18.5 % under the $PM_{2.5}$ concentration larger than 250 $\mu g\,m^{-3}$). The different variations of species percentage in total ions indicate that SO_4^{2-} and NH_4^+ may contribute more to the $PM_{2.5}$ pollution. This result is similar with the conclusion of Wang et al. (2014a), who considered the increasing proportion of sulfate enhanced particle hygroscopicity and thereby accelerating formation of the haze pollution.

3.2 Ratio of $[NO_3^-]/[SO_4^{2-}]$

The mass ratio of $[NO_3^-]/[SO_4^{2-}]$ has been used as an indicator of the relative importance of stationary vs. mobile sources of sulfur and nitrogen in the atmosphere. Higher $[NO_3^-]/[SO_4^{2-}]$ mass ratios indicate the predominance of mobile sources over stationary sources of pollutants (Arimoto et al., 1996).

The average mass ratio of $[NO_3^-]/[SO_4^{2-}]$ during the observation period was 0.68 ± 0.44, which was comparable with the results of Wang et al. (2014a), but higher than the

ACPD
15, 11111–11141, 2015

value measured during the winters of 2001–2003 in Beijing (0.49). Wang et al. (2005) suggested that the contribution of mobile sources (e.g., motor vehicles) increased in Beijing, in accord with the adjustment of the energy structure in recent years.

The $[NO_3^-]/[SO_4^{2-}]$ ratio was also classified according to the $PM_{2.5}$ concentration ranges. As shown in Fig. 6, we can find that the $[NO_3^-]/[SO_4^{2-}]$ ratio decrease with the increase of $PM_{2.5}$ level. When the $PM_{2.5}$ concentrations were lower than $75\,\mu g\,m^{-3}$, the ratio were larger than 1, indicating predominance of mobile source over stationary source of pollutants. When $PM_{2.5}$ concentration increased, the stationary sources would contribute more pollutants than mobile sources. The results also confirmed that SO_4^{2-} was one of the most important compositions which contributed to the $PM_{2.5}$ heavy pollution.

3.3 Diurnal variation

The diurnal variations of ion species in $PM_{2.5}$ in the sampling period were shown in Fig. 7. On the whole, SO_4^{2-}, NO_3^-, Cl^-, K^+ and NH_4^+ exhibited similar diurnal patterns with a broad nighttime maximum and a relatively low concentration at daytime, while the variations of Na^+, Mg^{2+} and Ca^{2+} were small. Compared with another highly resolved measurements for ion species at the same site during summer of 2008 (Gao et al., 2013), the diurnal cycle of SO_4^{2-} in this study was completely opposite, i.e., the highest concentration of SO_4^{2-} occurred at daytime and the lowest at night during summer campaign of 2008. Also, for some ions, such as SO_4^{2-}, Cl^- and K^+, high levels at night and low concentrations at daytime could be the characterizations of coal combustion. The sampling site is located outside the 5th ring of Beijing, and there still exists considerable coal combustion boilers for domestic heating. The emission from these coal combustion facilities would be one of the important reasons that led to the diurnal variations.

Gao et al. (2013) found the SO_4^{2-} concentrations in summer rapidly increased from the early morning to the late afternoon synchronously with the enhancement of solar

ACPD
15, 11111–11141, 2015

radiation and the O_3 and SO_2 concentrations. In this study, the O_3 concentration was low, especially in the pollution episodes ($< 15\,\mu g\,m^{-3}$) (Wang et al., 2014a). Such low O_3 levels cannot supply enough oxidizing capacity in the atmosphere; therefore, other oxidation reactions, regional transport at night or the impact of meteorological may also be responsible for the high levels of SO_4^{2-}, NH_4^+ and NO_3^-.

3.4 The speciation of major ions

The chemical forms of those major ions, i.e. SO_4^{2-}, NO_3^-, Cl, NH_4^+, Ca^{2+}, and K^+, in aerosols in Beijing were identified by bivariate correlations. Verma et al. (2010) and Wang et al. (2005) used bivariate correlations to identify the possible chemical forms of ions in $PM_{2.5}$. Since concentrations of all the ions are not normally distributed (k-s test, $p < 0.05$), Spearman Correlation analysis was applied. Table 5 showed the correlation coefficients among these major ions.

Ammonia is an important alkaline gas in the atmosphere. Ammonia in air is neutralized first by H_2SO_4 to form $(NH_4)_2SO_4$ or NH_4HSO_4, and then the remaining is neutralized by reaction with HNO_3 to form NH_4-NO_3.

In this study, among all cations, NH_4^+ was highly significantly correlated with NO_3^- and SO_4^{2-} as shown in Table 6. The slope of the regression between NH_4^+ and SO_4^{2-} (μeq vs. μeq) for the whole data set was 1.33, indicating the complete neutralization of SO_4^{2-} by NH_4^+, and suggested that $(NH_4)_2SO_4$, instead of NH_4HSO_4, was the major species formed by SO_4^{2-} and NH_4^+. Moreover, the slope between NH_4^+ and the sum of SO_4^{2-} and NO_3^- (μeq vs. μeq) was 0.99, further revealing NH_4^+ completely neutralized by both SO_4^{2-} and NO_3^-. Thus only Cl^- can supply negative charge to balance the Na^+, K^+. Considering the correlation coefficients of Cl^- between Na^+, K^+, were comparable, the mixture of NaCl and KCl were likely to be the major form of ions $(NH_4)_2SO_4$ and NH_4NO_3.

ACPD
15, 11111–11141, 2015

3.5 Source analysis

The mass concentrations of all ions species were input into EPA PMF 4.2 model to identify the potential sources. Four factors were isolated, representing potential sources, including secondary nitrate, secondary sulfate, coal combustion and biomass burning, and fugitive dust. The factor profiles of $PM_{2.5}$ bound ion species at the monitoring site are shown in Fig. 8.

Factor 1 and factor 2 were considered as secondary nitrate and sulfate, with high loading of NO_3^- and NH_4^+ in factor 1, as well as SO_4^{2-} and NH_4^+ in factor 2. NO_3^- is mainly converted from ambient NO_x, which is emitted by both vehicle exhaust and fossil fuel combustion. The precursor of aerosol SO_4^{2-} is SO_2, which may originate from biomass burning and fossil fuel combustion. Cl^- and K^+ were found to be the main contributors to factor 3, originating mainly from coal and biomass combustion. Factor 4 is identified as fugitive dust, such as soil dust, constructive dust, and paved or unpaved road dust, including high contributions of Ca^{2+} and Mg^{2+}.

The factor contributions to the ion concentrations are illustrated in Fig. 9. Factors 1 and 2 were the biggest contributors to NO_3^- and SO_4^{2-}, respectively. Both factors also comparably contribute to the concentration of NH_4^+. Factor 3 was the main source for Cl^- and K^+, while factors 1 and 2 also took some portions for Cl^- and K^+, respectively. Na^+, Mg^{2+} and Ca^{2+} were mostly contributed by factor 4.

4 Conclusions

In this study, we reported in-situ measurements of water-soluble inorganic ions associated with $PM_{2.5}$ at an urban site of Beijing during the air pollution episode in January 2013. The hourly concentrations of Cl^-, NO_3^-, SO_4^{2-}, Na^+, NH_4^+, K^+, Mg^{2+} and Ca^{2+} were measured.

Peak concentrations of the ions were observed in four periods (10–15, 18–20, 21–24, and 26–30 January). SO_4^{2-} and NO_3^- exhibited high concentrations in three periods.

ACPD
15, 11111–11141, 2015

Meanwhile, the percentage of SO_4^{2-} in total ions concentrations kept an increasing trend with the enhancement of $PM_{2.5}$ concentration, thus high concentrations of SO_4^{2-} and NH_4^+ can be considered as one of the main reasons of air pollution episodes. NH_4^+ also played an important role in the formation of $PM_{2.5}$. Based on the correlation analysis, the observed ions existed mainly in the form of $(NH_4)_2SO_4$, NH_4NO_3, NaCl and KCl in aerosol particles.

The ratio of $[NO_3^-]/[SO_4^{2-}]$ also proved the role of SO_4^{2-} in the air pollution episodes. With the aggravation of air quality, the $[NO_3^-]/[SO_4^{2-}]$ displayed a decreasing trend, indicating the SO_2 emitters, such as some stationary sources, contributed more to $PM_{2.5}$ aerosols formation, rather than mobile sources, which are considered as the sources of NO_3^-.

Obvious diurnal variations of SO_4^{2-}, NO_3^-, NH_4^+ were observed. All of them exhibited similar patterns with high concentration in night and relatively low level at daytime. Considering the lack of strong oxidative atmosphere during monitoring period, pollutant transport at night may be responsible for the high level of SO_4^{2-}, NH_4^+ and NO_3^-.

Potential sources were identified by applying PMF. Secondary nitrate, secondary sulfate, coal combustion and biomass burning, as well as fugitive dust were considered as the major contributors to total ions.

Acknowledgement. This study was funded by "National Basic Research Program of China" (Grants No. 2011CB503801) and Beijing Natural Science Foundation (8121002).

References

Arimoto, R., Duce, R. A., Savoie, D. L., Prospero, J. M., Talbot, R., Cullen, J. D., Tomza, U., Lewis, N. F., and Ray, B. J.: Relationships among aerosol constituents from Asia and the North Pacific during PEM-West A, J. Geophys. Res.-Atmos., 101, 2011–2023, doi:10.1029/95jd01071, 1996.

ACPD
15, 11111–11141, 2015

Cao, J.-J., Shen, Z.-X., Chow, J. C., Watson, J. G., Lee, S.-C., Tie, X.-X., Ho, K.-F., Wang, G.-H., and Han, Y.-M.: Winter and summer $PM_{2.5}$ chemical compositions in fourteen Chinese cities, JAPCA J. Air Waste Ma., 62, 1214–1226, doi:10.1080/10962247.2012.701193, 2012.
Chen, R. J., Zhao, Z. H., and Kan, H. D.: Heavy smog and hospital visits in Beijing, China, Am. J. Resp. Crit. Care, 188, 1170–1171, 2013.
Duan, F. K., Liu, X. D., He, K. B., Lu, Y. Q., and Wang, L.: Atmospheric aerosol concentration level and chemical characteristics of water-soluble ionic species in wintertime in Beijing, China, J. Environ. Monitor., 5, 569–573, doi:10.1039/b303691j, 2003.
Duan, F. K., Liu, X. D., Yu, T., and Cachier, H.: Identification and estimate of biomass burning contribution to the urban aerosol organic carbon concentrations in Beijing, Atmos. Environ., 38, 1275–1282, doi:10.1016/j.atmosenv.2003.11.037, 2004.
Gao, X., Nie, W., Xue, L., Wang, T., Wang, X., Gao, R., Wang, W., Yuan, C., Gao, J., Ravi, K. P., Wang, J., and Zhang, Q.: Highly time-resolved measurements of secondary ions in $PM_{2.5}$ during the 2008 Beijing Olympics: the impacts of control measures and regional transport, Aerosol Air Qual. Res., 13, 367–376, doi:10.4209/aaqr.2012.04.0083, 2013.
He, K., Yang, F., Ma, Y., Zhang, Q., Yao, X., Chan, C. K., Cadle, S., Chan, T., and Mulawa, P.: The characteristics of $PM_{2.5}$ in Beijing, China, Atmos. Environ., 35, 4959–4970, doi:10.1016/S1352-2310(01)00301-6, 2001.
Hu, G., Zhang, Y., Sun, J., Zhang, L., Shen, X., Lin, W., and Yang, Y.: Variability, formation and acidity of water-soluble ions in $PM_{2.5}$ in Beijing based on the semi-continuous observations, Atmos. Res., 145–146, 1–11, doi:10.1016/j.atmosres.2014.03.014, 2014.
Huang, K., Zhuang, G., Wang, Q., Fu, J. S., Lin, Y., Liu, T., Han, L., and Deng, C.: Extreme haze pollution in Beijing during January 2013: chemical characteristics, formation mechanism and role of fog processing, Atmos. Chem. Phys. Discuss., 14, 7517–7556, doi:10.5194/acpd-14-7517-2014, 2014.
Huang, X.-F., He, L.-Y., Hu, M., Canagaratna, M. R., Sun, Y., Zhang, Q., Zhu, T., Xue, L., Zeng, L.-W., Liu, X.-G., Zhang, Y.-H., Jayne, J. T., Ng, N. L., and Worsnop, D. R.: Highly time-resolved chemical characterization of atmospheric submicron particles during 2008 Beijing Olympic Games using an Aerodyne High-Resolution Aerosol Mass Spectrometer, Atmos. Chem. Phys., 10, 8933–8945, doi:10.5194/acp-10-8933-2010, 2010.
Ji, D., Li, L., Wang, Y., Zhang, J., Cheng, M., Sun, Y., Liu, Z., Wang, L., Tang, G., Hu, B., Chao, N., Wen, T., and Miao, H.: The heaviest particulate air-pollution episodes occurred

ACPD
15, 11111–11141, 2015

in northern China in January 2013: insights gained from observation, Atmos. Environ., 92, 546–556, doi:10.1016/j.atmosenv.2014.04.048, 2014.
Liu, Y., Li, W. L., and Zhou, X. J.: Simulation of secondary aerosols over North China in summer, Sci. China Ser. D, 48, 185–195, doi:10.1360/05yd0405, 2005.
Ocskay, R., Salma, I., Wang, W., and Maenhaut, W.: Characterization and diurnal variation of size-resolved inorganic water-soluble ions at a rural background site, J. Environ. Monitor., 8, 300–306, doi:10.1039/b513915e, 2006.
Ouyang, Y.: China wakes up to the crisis of air pollution, The Lancet Respiratory Medicine, 1, 12, doi:10.1016/S2213-2600(12)70065-6, 2013.
Pathak, R. K., Wu, W. S., and Wang, T.: Summertime $PM_{2.5}$ ionic species in four major cities of China: nitrate formation in an ammonia-deficient atmosphere, Atmos. Chem. Phys., 9, 1711–1722, doi:10.5194/acp-9-1711-2009, 2009.
Shon, Z.-H., Kim, K.-H., Song, S.-K., Jung, K., Kim, N.-J., and Lee, J.-B.: Relationship between water-soluble ions in $PM_{2.5}$ and their precursor gases in Seoul megacity, Atmos. Environ., 59, 540–550, doi:10.1016/j.atmosenv.2012.04.033, 2012.
Su, F. Q., Gao, Q. X., Zhang, Z. G., Ren, Z. H., and Yang, X. X.: Transport pathways of pollutants from outside in atmosphere boundary layer (in Chinese with English abstract), Res. Environ. Sci., 17, 26–40, 2004.
Sun, Y. L., Wang, Z. F., Fu, P. Q., Yang, T., Jiang, Q., Dong, H. B., Li, J., and Jia, J. J.: Aerosol composition, sources and processes during wintertime in Beijing, China, Atmos. Chem. Phys., 13, 4577–4592, doi:10.5194/acp-13-4577-2013, 2013.
Vedantham, R., Landis, M. S., Olson, D., and Pancras, J. P.: Source identification of $PM_{2.5}$ in Steubenville, Ohio using a hybrid method for highly time-resolved data, Environ. Sci. Technol., 48, 1718–1726, doi:10.1021/es402704n, 2014.
Verma, S. K., Deb, M. K., Suzuki, Y., and Tsai, Y. I.: Ion chemistry and source identification of coarse and fine aerosols in an urban area of eastern central India, Atmos. Res., 95, 65–76, doi:10.1016/j.atmosres.2009.08.008, 2010.
Wang, W., Primbs, T., Tao, S., and Simonich, S. L. M.: Atmospheric particulate matter pollution during the 2008 Beijing Olympics, Environ. Sci. Technol., 43, 6440–6440, doi:10.1021/es901953s, 2009.
Wang, Y., Zhuang, G. S., Tang, A. H., Yuan, H., Sun, Y. L., Chen, S. A., and Zheng, A. H.: The ion chemistry and the source of $PM_{2.5}$ aerosol in Beijing, Atmos. Environ., 39, 3771–3784, doi:10.1016/j.atmosenv.2005.03.013, 2005.

ACPD
15, 11111–11141, 2015

Wang, Y., Yao, L., Wang, L., Liu, Z., Ji, D., Tang, G., Zhang, J., Sun, Y., Hu, B., and Xin, J.: Mechanism for the formation of the January 2013 heavy haze pollution episode over central and eastern China, Sci. China Ser. D, 57, 14–25, doi:10.1007/s11430-013-4773-4, 2014a.

Wang, Z., Li, J., Wang, Z., Yang, W., Tang, X., Ge, B., Yan, P., Zhu, L., Chen, X., Chen, H., Wand, W., Li, J., Liu, B., Wang, X., Zhao, Y., Lu, N., and Su, D.: Modeling study of regional severe hazes over mid-eastern China in January 2013 and its implications on pollution prevention and control, Sci. China Ser. D, 57, 3–13, doi:10.1007/s11430-013-4793-0, 2014b.

Xue, J., Lau, A. K. H., and Yu, J. Z.: A study of acidity on $PM_{2.5}$ in Hong Kong using online ionic chemical composition measurements, Atmos. Environ., 45, 7081–7088, doi:10.1016/j.atmosenv.2011.09.040, 2011.

Yao, X., Chan, C. K., Fang, M., Cadle, S., Chan, T., Mulawa, P., He, K., and Ye, B.: The water-soluble ionic composition of $PM_{2.5}$ in Shanghai and Beijing, China, Atmos. Environ., 36, 4223–4234, doi:10.1016/S1352-2310(02)00342-4, 2002.

Ye, B., Ji, X., Yang, H., Yao, X., Chan, C. K., Cadle, S. H., Chan, T., and Mulawa, P. A.: Concentration and chemical composition of $PM_{2.5}$ in Shanghai for a 1-year period, Atmos. Environ., 37, 499–510, doi:10.1016/S1352-2310(02)00918-4, 2003.

Zhang, Q. H., Zhang, J. P., and Xue, H. W.: The challenge of improving visibility in Beijing, Atmos. Chem. Phys., 10, 7821–7827, doi:10.5194/acp-10-7821-2010, 2010.

Zhang, R., Jing, J., Tao, J., Hsu, S.-C., Wang, G., Cao, J., Lee, C. S. L., Zhu, L., Chen, Z., Zhao, Y., and Shen, Z.: Chemical characterization and source apportionment of $PM_{2.5}$ in Beijing: seasonal perspective, Atmos. Chem. Phys., 13, 7053–7074, doi:10.5194/acp-13-7053-2013, 2013.

Zhang, R., Li, Q., and Zhang, R.: Meteorological conditions for the persistent severe fog and haze event over eastern China in January 2013, Sci. China Ser. D, 57, 26–35, doi:10.1007/s11430-013-4774-3, 2014.

Zhao, P. S., Dong, F., He, D., Zhao, X. J., Zhang, X. L., Zhang, W. Z., Yao, Q., and Liu, H. Y.: Characteristics of concentrations and chemical compositions for PM2.5 in the region of Beijing, Tianjin, and Hebei, China, Atmos. Chem. Phys., 13, 4631–4644, doi:10.5194/acp-13-4631-2013, 2013.

ACPD
15, 11111–11141, 2015

Table 1. Meteorological conditions of January in Beijing.

Meteorological parameter	Temperature (°C)	Relative humidity (%)	Atmospheric press (Hpa)	Wind speed ($m s^{-1}$)	Calm wind frequency (%)
Mean (range)	−5.1 (−14.0–3.8)	55 (18–94)	1023.7 (1012.8–1041.8)	1.9 (0–7.9)	6.64

ACPD
15, 11111–11141, 2015

Table 2. The detection limit of URG9000.

Ions	Cl^-	NO_3^-	SO_4^{2-}	Na^+	NH_4^+	K^+	Mg^{2+}	Ca^{2+}
DL ($\mu g\,m^{-3}$)	0.0100	0.0500	0.0400	0.0500	0.0500	0.0900	0.0600	0.1000

ACPD
15, 11111–11141, 2015

Table 3. Descriptive statistics of ion species in January (N = 676, μg m^{-3}).

Species	Mean	Median	Range	Percentile		
				25 %	50 %	75 %
Cl^-	4.91	3.71	0.28–21.90	1.69	3.71	6.96
NO_3^-	16.35	12.27	1.39–66.11	3.94	12.27	25.71
SO_4^{2-}	23.52	9.14	0.01–179.44	2.46	9.14	41.32
Na^+	2.04	1.93	0.86–8.22	1.66	1.93	2.28
NH_4^+	10.48	6.25	0.29–165.26	1.63	6.25	15.01
K^+	1.38	1.02	0.07–9.53	0.36	1.02	1.93
Mg^{2+}	0.71	0.73	0.13–1.04	0.69	0.73	0.80
Ca^{2+}	1.08	1.15	0.07–2.62	1.05	1.15	1.25

ACPD
15, 11111–11141, 2015

Table 4. Comparisons of the concentrations of ions in several studies in Beijing during winter by manual samplers ($\mu g\,m^{-3}$).

Studies	Sampling time	SO_4^{2-}	NO_3^-	Cl^-	NH_4^+
He et al. (2001)	1999–2000	24.87	15.35	–	7.80
Cao et al. (2012)	Jan 2003	20.0	13.1	2.3	9.4
Sun et al. (2004)	2002–2003	27.80	16.60	6.77	15.50
Wang et al. (2005)	2001–2003	20.96	12.29	5.28	10.64
Okuda et al. (2013)	2008–2009	24.09	18.71	8.06	12.26
Zhao et al. (2013)	2009–2010	14.23	17.09	–	5.21
This study	Jan 2013	23.52	16.35	4.91	10.48

ACPD
15, 11111–11141, 2015

Table 5. Comparisons of the concentrations of ions between this study and a simultaneous study ($\mu g\,m^{-3}$).

	Huang et al. (2014)		This study	
	4–9 Jan	10–15 Jan	4–9 Jan	10–15 Jan
Cl^-	2.89	7.57	2.35	8.63
NO_3^-	6.88	28.58	5.35	24.36
SO_4^{2-}	7.81	44.32	3.75	47.52
Na^+	0.57	0.95	1.78	2.56
NH_4^+	4.34	14.64	1.76	16.28
K^+	0.81	4.15	0.49	2.45
Mg^{2+}	0.23	0.23	0.73	0.78
Ca^{2+}	0.51	0.44	1.25	1.28

ACPD
15, 11111–11141, 2015

Table 6. The correlation coefficients (r) and the linear regression equations between major ions.

	Cl^-	NO_3^-	SO_4^{2-}	
Na^+	**0.900**	**0.827**	**0.818**	
NH_4^+	**0.895**	**0.971**	**0.970**	$(NH_4^+) = 1.33 \times (SO_4^{2-}) - 0.01$
K^+	**0.892**	**0.903**	**0.924**	$(NH_4^+) = 3.40 \times (NO_3^-) - 0.25$
Mg^{2+}	0.182	0.021	0.071	$(NH_4^+) = 0.99 \times [(SO_4^{2-}) + (NO_3^-)] - 0.01$
Ca^{2+}	0.075	−0.170	−0.145	

Note: bold figures indicates that the correlation coefficient is higher than 0.80.

ACPD
15, 11111–11141, 2015

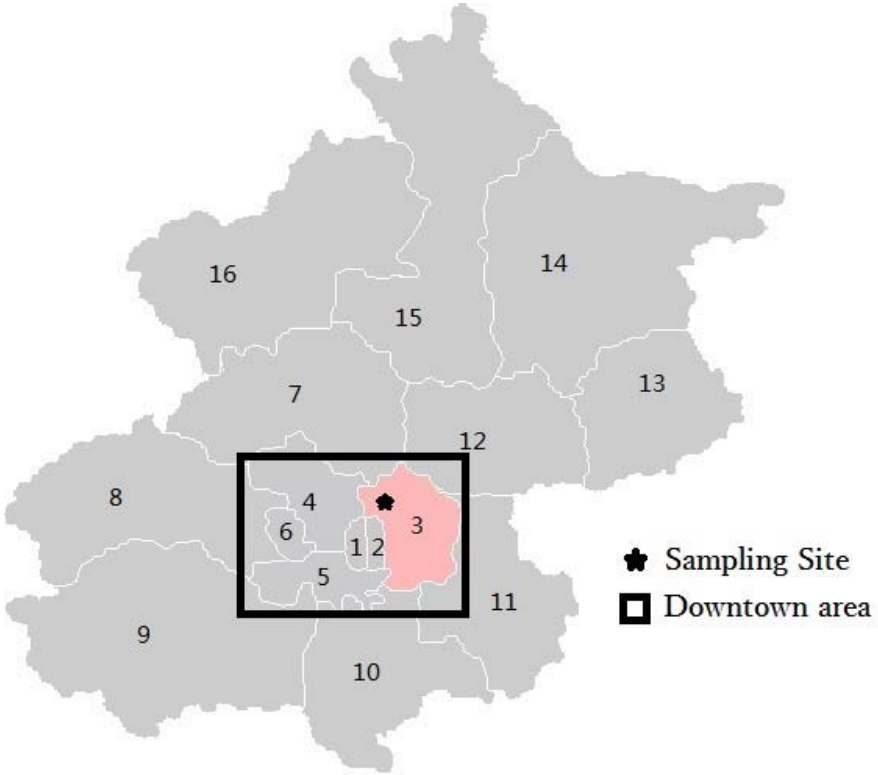

Figure 1. Location of sampling site in Beijing ((1) Xicheng District; (2) Dongcheng District; (3) Chaoyang District; (4) Haidian District; (5) Fengtai District; (6) Shijingshan District; (7) Changping District; (8) Mentougou District; (9) Fangshan District; (10) Daxing District; (11) Tongzhou District; (12) Shunyi District; (13) Pinggu District; (14) Miyun District; (15) Huairou District; (16) Yanqin District).

ACPD
15, 11111–11141, 2015

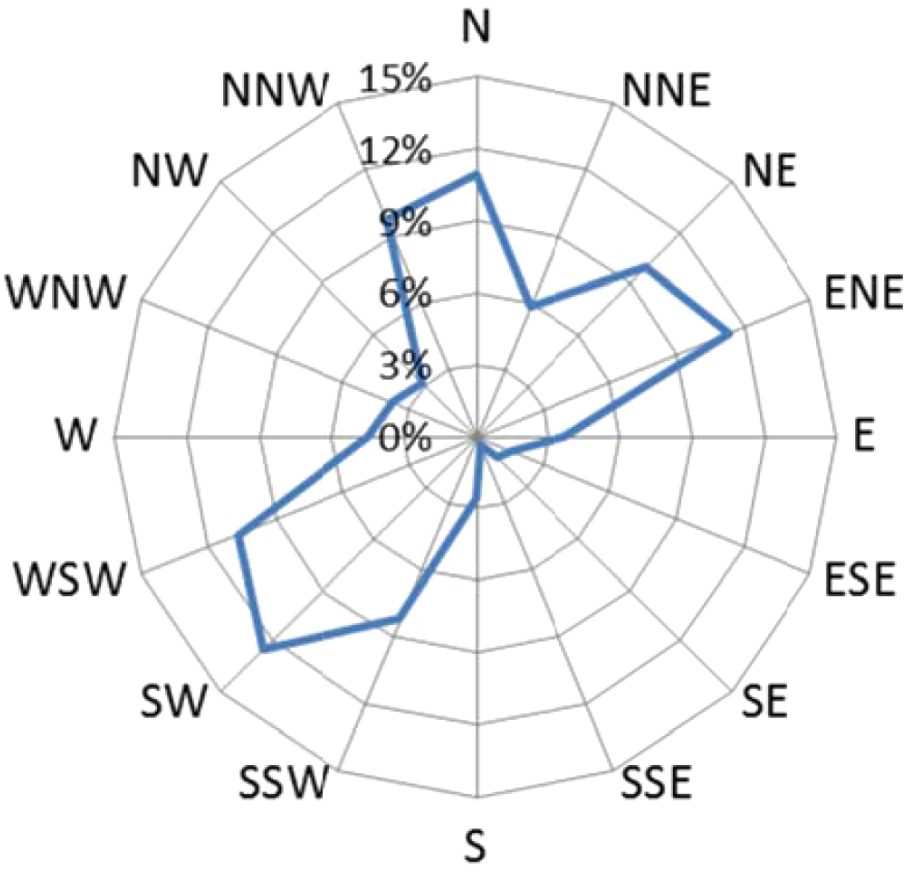

Figure 2. Wind roses of January in Beijing.

ACPD
15, 11111–11141, 2015

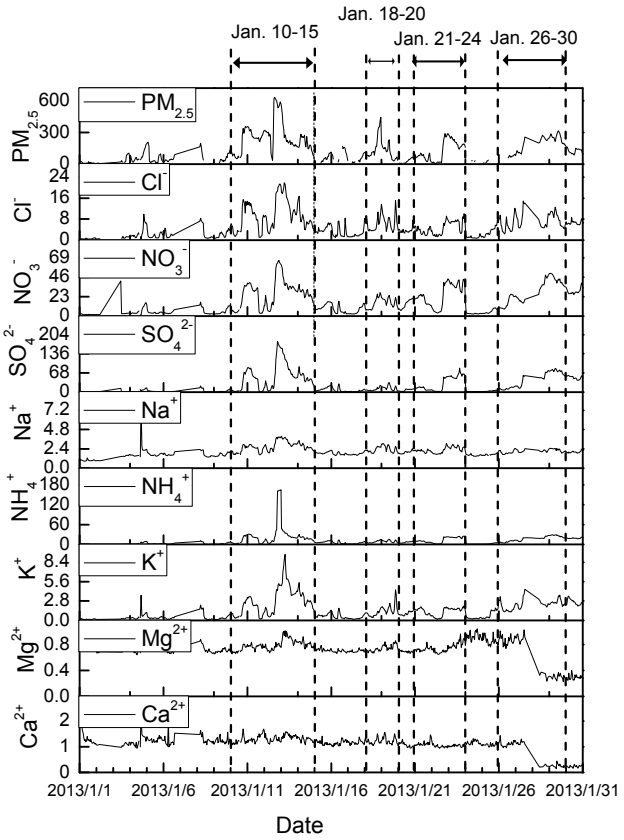

Figure 3. Variation of $PM_{2.5}$ and ions concentrations in the sampling site in January 2013 (the peak period of $PM_{2.5}$ are marked between the dote lines).

ACPD
15, 11111–11141, 2015

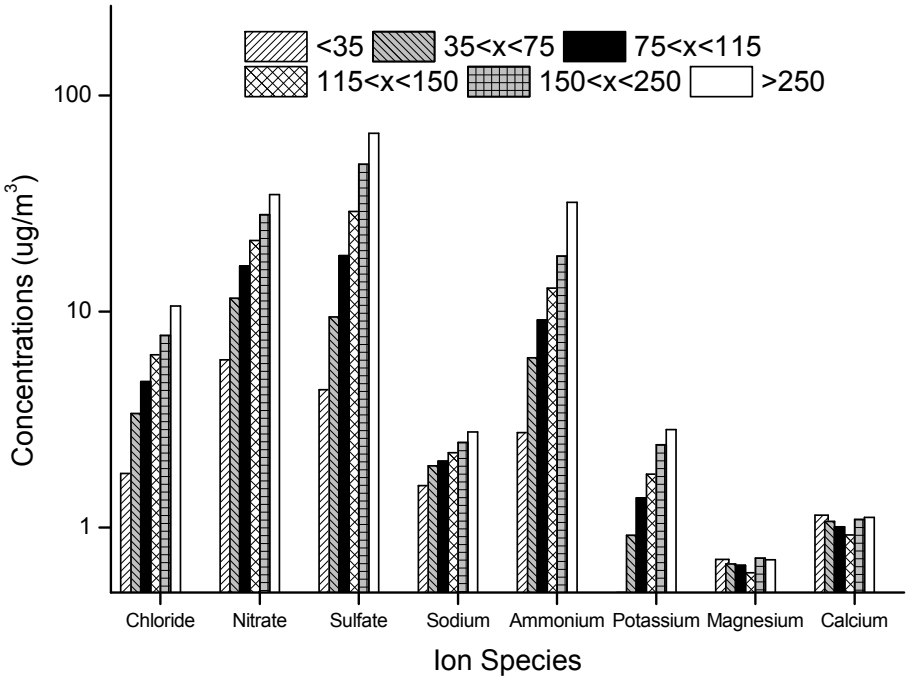

Figure 4. Concentrations of ion species at different $PM_{2.5}$ range.

ACPD
15, 11111–11141, 2015

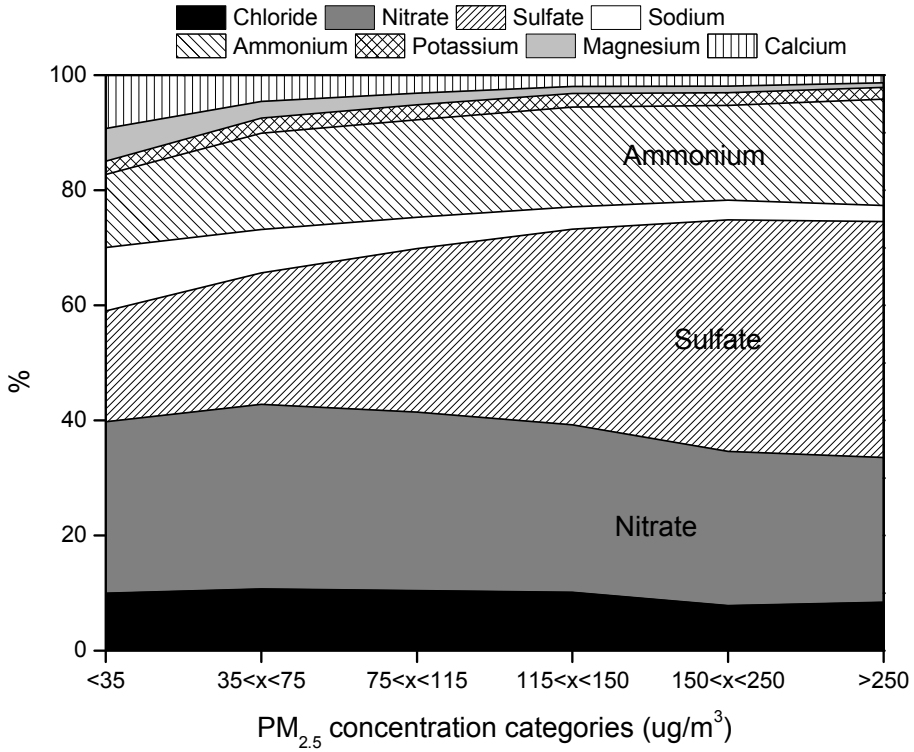

Figure 5. Percentage of ion species in total ions at different $PM_{2.5}$ range.

ACPD
15, 11111–11141, 2015

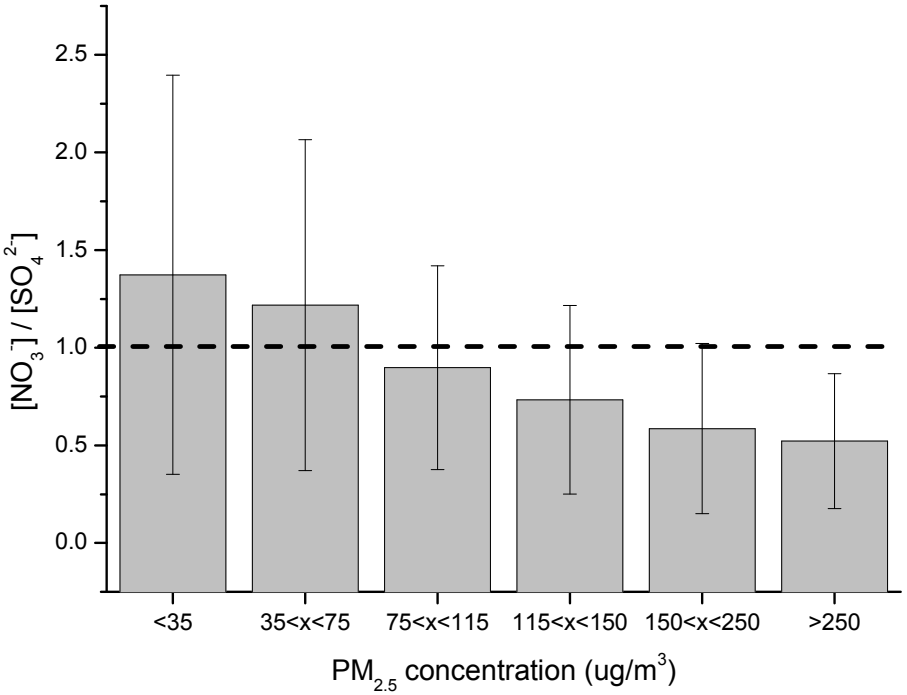

Figure 6. Ratio of $[NO_3^-]/[SO_4^{2-}]$ at different $PM_{2.5}$ concentration ranges.

ACPD
15, 11111–11141, 2015

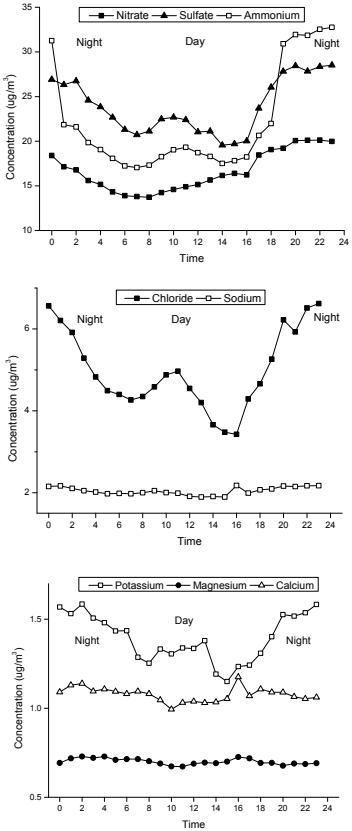

Figure 7. Diurnal variations of ion species.

ACPD
15, 11111–11141, 2015

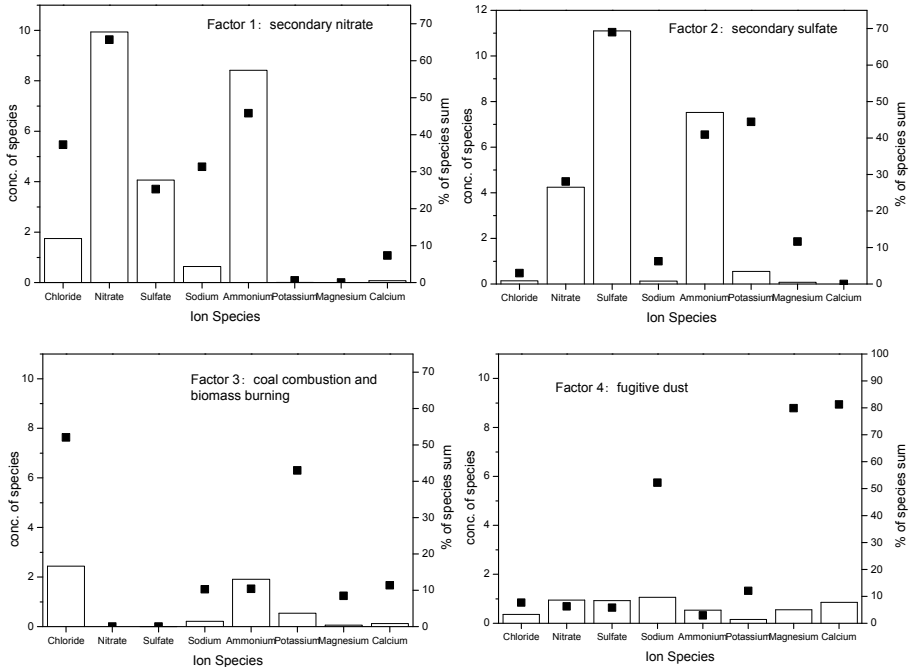

Figure 8. Factor profiles of $PM_{2.5}$ bound ion species in the urban site of Beijing.

ACPD
15, 11111–11141, 2015

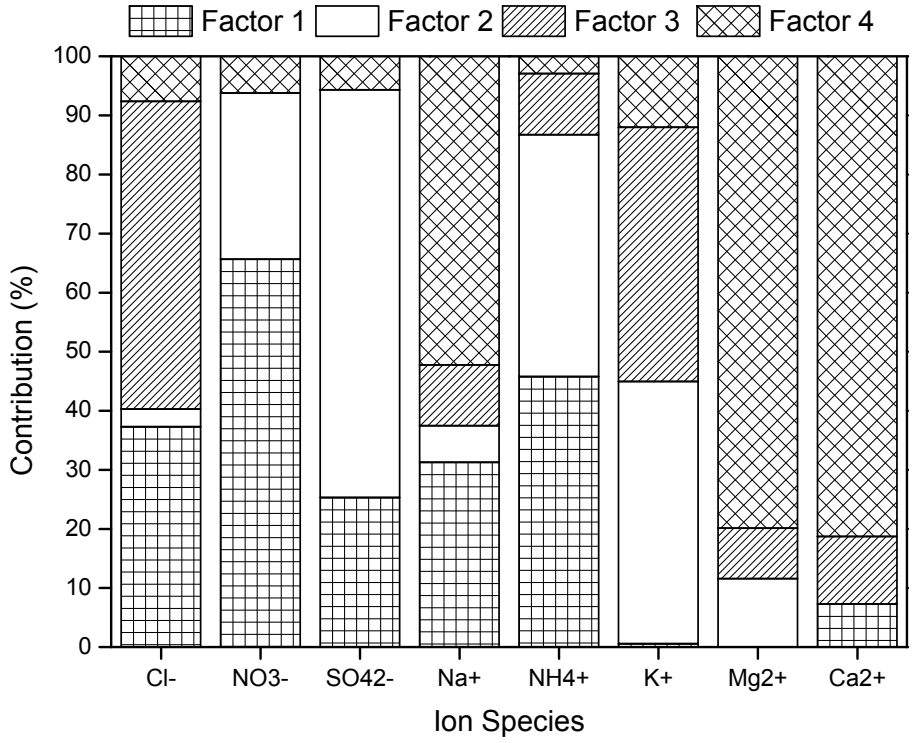

Figure 9. The contributions of factors to the ion species.

ACPD
15, 11111–11141, 2015